University of Montana

ScholarWorks at University of Montana

Chemistry and Biochemistry Faculty
Publications

Chemistry and Biochemistry

Tropospheric Carbon Monoxide Measurements from the Scanning High-Resolution Interferometer Sounder on 7 September 2000 in Southern Africa During SAFARI 2000

W. W. McMillan
University of Maryland - Baltimore County

M. L. McCourt
University of Maryland - Baltimore County

H. E. Revercomb
University of Wisconsin - Madison

R. O. Knuteson
University of Wisconsin - Madison

Ted J. Christian
University of Montana - Missoula

See next page for additional authors

Follow this and additional works at: https://scholarworks.umt.edu/chem_pubs

🎨 Part of the Biochemistry Commons, and the Chemistry Commons

Let us know how access to this document benefits you.

Recommended Citation

McMillan, W. W., et al., Tropospheric carbon monoxide measurements from the Scanning High-Resolution Interferometer Sounder on 7 September 2000 in southern Africa during SAFARI 2000, J. Geophys. Res., 108(D13), 8492, doi:10.1029/2002JD002335, 2003.

Authors

W. W. McMillan, M. L. McCourt, H. E. Revercomb, R. O. Knuteson, Ted J. Christian, B. G. Doddridge, Peter V. Hobbs, J. V. Lukovich, P. C. Novelli, S. J. Piketh, L. Sparling, D. Stein, R. J. Swap, and Robert J. Yokelson

Tropospheric carbon monoxide measurements from the Scanning High-Resolution Interferometer Sounder on 7 September 2000 in southern Africa during SAFARI 2000

W. W. McMillan,[1] M. L. McCourt,[1] H. E. Revercomb,[2] R. O. Knuteson,[2] T. J. Christian,[3] B. G. Doddridge,[4] P. V. Hobbs,[5] J. V. Lukovich,[6] P. C. Novelli,[7] S. J. Piketh,[8] L. Sparling,[1] D. Stein,[9] R. J. Swap,[9] and R. J. Yokelson[3]

[1]   Retrieved tropospheric carbon monoxide (CO) column densities are presented for more than 9000 spectra obtained by the University of Wisconsin-Madison (UWis) Scanning High-Resolution Interferometer Sounder (SHIS) during a flight on the NASA ER-2 on 7 September 2000 as part of the Southern African Regional Science Initiative (SAFARI 2000) dry season field campaign. Enhancements in tropospheric column CO were detected in the vicinity of a controlled biomass burn in the Timbavati Game Reserve in northeastern South Africa and over the edge of the *river of smoke* in south central Mozambique. Relatively clean air was observed over the far southern coast of Mozambique. Quantitative comparisons are presented with in situ measurements from five different instruments flying on two other aircraft: the University of Washington Convair-580 (CV) and the South African Aerocommander JRB in the vicinity of the Timbavati fire. Measured tropospheric CO columns (extrapolated from 337 to 100 mb) of 2.1×10^{18} cm^{-2} in background air and up to 1.5×10^{19} cm^{-2} in the smoke plume agree well with SHIS retrieved tropospheric CO columns of $(2.3 \pm 0.25) \times 10^{18}$ cm^{-2} over background air near the fire and $(1.5 \pm 0.35) \times 10^{19}$ cm^{-2} over the smoke plume. Qualitative comparisons are presented with three other in situ CO profiles obtained by the South African JRA aircraft over Mozambique and northern South Africa showing the influence of the *river of smoke*.   INDEX TERMS: 0322 Atmospheric Composition and Structure: Constituent sources and sinks; 0345 Atmospheric Composition and Structure: Pollution—urban and regional (0305); 0365 Atmospheric Composition and Structure: Troposphere—composition and chemistry; 0368 Atmospheric Composition and Structure: Troposphere—constituent transport and chemistry

1.   Introduction

[2]   With 50% or more of its tropospheric abundance derived from anthropogenic sources and a lifetime of 1–6 months, carbon monoxide (CO) serves as an indicator of human influence and an excellent tracer of tropospheric transport [*Sze*, 1977; *Crutzen et al.*, 1979; *Law and Pyle*, 1993; *Badr and Probert*, 1994]. As a main sink for OH, CO also plays a critical role in tropospheric chemistry [*Sze*,

1977; *Logan et al.*, 1981; *Thompson*, 1992]. Although fossil fuel burning dominates the anthropogenic source of CO in the Northern Hemisphere, the dominant anthropogenic source in the Southern Hemisphere, particularly in southern Africa, is biomass burning [*Otter et al.*, 1997]. Remote sensing observations of CO from biomass burning in Africa, South America, and Indonesia were a major achievement of the first satellite-derived global view provided by the MAPS instrument flying onboard the space shuttle [*Reichle et al.*, 1982, 1986, 1990, 1999; *Reichle and Connors*, 1999;

---

[1]Physics Department, University of Maryland Baltimore County, Baltimore, Maryland, USA.
[2]Cooperative Institute for Meteorological Satellite Studies, University of Wisconsin, Madison, Wisconsin, USA.
[3]Department of Chemistry, University of Montana, Missoula, Montana, USA.
[4]Department of Meteorology, University of Maryland, College Park, Maryland, USA.

[5]Cloud and Aerosol Research Group, Department of Atmospheric Sciences, University of Washington, Seattle, Washington, USA.
[6]Joint Center for Earth Systems Technology, University of Maryland Baltimore County, Baltimore, Maryland, USA.
[7]Climate Monitoring and Diagnostics Laboratory, National Oceanic and Atmospheric Administration (NOAA), Boulder, Colorado, USA.
[8]Climatology Research Group, University of Witswatersrand, Johannesburg, South Africa.
[9]Department of Environmental Sciences, University of Virginia, Charlottesville, Virginia, USA.

Connors et al., 1991b, 1996, 1999; *Christopher et al.*, 1998; *Newell et al.*, 1999].

[3] Recent trends in lower tropospheric CO point to decreasing CO [*Novelli et al.*, 1998a; *Khalil and Rasmussen*, 1994] after increasing trends were observed in the early 1980s [*Khalil and Rasmussen*, 1988]. No significant CO trends have been observed in the Southern Hemisphere [*Scheel et al.*, 1998; *Brunke et al.*, 1990]. However, *Yurganov et al.* [1997] partially attribute an increasing trend in tropospheric CO over Russia to forest fires. The ancient roots of biomass burning agricultural practices, discontinued in Europe approximately 1000 years ago, flourish in the slash and burn methods practiced today in southern Africa [*Crutzen and Andreae*, 1990]. Nevertheless, increasing population and modernization could lead to increases in both fossil fuel and domestic burning as sources for CO. Whether or not the large-scale savanna burning increases in southern Africa remains to be seen.

[4] Previous scientific campaigns explored the impact of biomass burning on tropospheric chemistry including CITE 3 [*Andreae et al.*, 1994], TROPOZ II [*Roths and Harris*, 1996; *Jonquiéres and Marenco*, 1998], GTE TRACE-A [*Thompson et al.*, 1996], SAFARI 92 [*Thompson et al.*, 1996; *Lindesay et al.*, 1996], PEM TRACE-A [*Pougatchev et al.*, 1999], TRACE-B [*Coleman et al.*, 2001], and correlative measurements for validation of MAPS [*Connors et al.*, 1991a; *Novelli et al.*, 1998b; *Pougatchev et al.*, 1998]. The resulting analyses and models clearly show the impact of biomass burning on the Southern Hemisphere [*Thompson et al.*, 1996; *Pickering et al.*, 1996; *Chatfield et al.*, 1998] and southern Africa in particular [*Chatfield et al.*, 1996; *Scholes et al.*, 1996; *Cofer et al.*, 1996; *Piketh et al.*, 1999; *Kirkman et al.*, 2000]. Ongoing satellite monitoring of the effects of biomass burning on tropical tropospheric ozone [*Thompson et al.*, 2001, 2000] and aerosols [*Herman et al.*, 1997; *Torres et al.*, 1998] have been performed with observations from the Total Ozone Mapping Spectrometer (TOMS).

[5] All these observations illustrate the effects of biomass burning beyond local scales and into the realm of regional transboundary and global pollution. Major modeling efforts are underway to assimilate CO observations into chemical transport models to study the dispersion of pollutants [*Clerbaux et al.*, 2001] and by inverse modeling to determine from where it comes [*Pak and Prather*, 2001]. Recent research points to the impacts of biomass burning beyond tropospheric chemistry and on to stratospheric moisture [*Sherwood*, 2002].

[6] The Southern African Regional Science Initiative (SAFARI 2000), conducted from 1999 to 2001, had as one of its main objectives the determination of aerosol and trace gas emissions over southern Africa from sources to impacts [*Annegarn et al.*, 2002; *Otter et al.*, 2002; *Swap et al.*, 2002a, 2002b]. Employing a nested approach of ground-based, airborne, and satellite-based observing platforms, SAFARI 2000 offers a number of rich data sets with which to study the emission, transport, and transformation of CO in the Southern Hemisphere. In support of the SAFARI 2000 dry season field campaign, the University of Wisconsin-Madison (UWis) Scanning High-Resolution Interferometer Sounder (SHIS) flew on the NASA ER-2 [*Moeller et al.*, 2003]. With a broad infrared spectral coverage (18–3.3 μm), SHIS produced simultaneous information regarding tropospheric temperature and moisture profiles, surface temperature and emissivity, cloud properties, and trace gas abundances including CO [*Moeller et al.*, 2003].

[7] Previous airborne FTIR remote sensing observations have been made of CO on a continental scale revealing synoptic controls on transport [*McMillan et al.*, 1997], of CO from forest fires [*Stearns et al.*, 1986; *Worden et al.*, 1997], and in forest fire smoke plumes [*McMillan et al.*, 1996; *Worden et al.*, 1997]. However, none of these studies occurred as part of an international effort to study as large and important an ecosystem as southern Africa. Moreover, no coordinated in situ measurements have been presented as part of such FTIR remote sensing observations.

[8] In this paper, we present the first detailed tropospheric CO retrievals from SHIS using a technique used previously for the earlier High-Resolution Interferometer Sounder (HIS) instrument [*McMillan et al.*, 1996, 1997]. Looking at a single flight during SAFARI 2000, we compare SHIS CO retrievals with in situ measurements for validation and spatial trends. Enhanced tropospheric CO is observed clearly near the Timbavati controlled burn and at the edge of the *river of smoke* over southern Mozambique. The *river of smoke* is the descriptive name given to the plume of biomass burning products swept from the southeastern coast of Africa out over the Indian Ocean between 31 August and 7 September 2000 (H. Annegarn et al., "The River of Smoke": Characteristics of the southern African springtime biomass burning haze, submitted to *Journal of Geophysical Research*, 2003, hereinafter referred to as Annegarn et al., submitted manuscript, 2003). The analysis of this flight represents the first step toward processing the 14 SAFARI 2000 flights of SHIS data and providing a full CO data set for validation of the Measurement of Pollution in the Troposphere (MOPITT) instrument which was onboard the NASA Terra spacecraft during SAFARI 2000.

2. SHIS and Spectra

[9] Originally envisioned for use onboard unmanned aerial vehicles (UAVs), mass and volume reductions coupled with improved electronics and detectors make SHIS much more versatile than the previously flown UWis HIS [*Moeller et al.*, 2003]. SHIS has flown in numerous NASA field experiments onboard both the NASA DC-8 and ER-2. However, the one SHIS flight analyzed in this paper does not take advantage of one of SHIS most significant improvements over HIS: cross-track scanning. Instead, when operated in a nadir viewing only mode, as for the 7 September 2000 flight, each succeeding SHIS field of view (FOV) overlaps the preceding one by approximately 92% [*Moeller et al.*, 2003].

[10] The SHIS, built by the UWis using an ABB Bomem, Inc. Fourier Transform Spectrometer (FTS) subassembly, covers a spectral range from 550 to 3000 cm^{-1} (18–3.3 μm) using three separate detectors sharing a common FOV. The FTS optical path difference (OPD) of approximately 1 cm provides an apodized spectral resolution of approximately 1 cm^{-1}. Although it possesses lower spatial resolution than other aircraft-based mapping instruments, such as the MODIS Airborne Simulator (MAS), SHIS considerably higher spectral resolution enables accurate simultaneous retrievals of atmospheric temperature and moisture profiles,
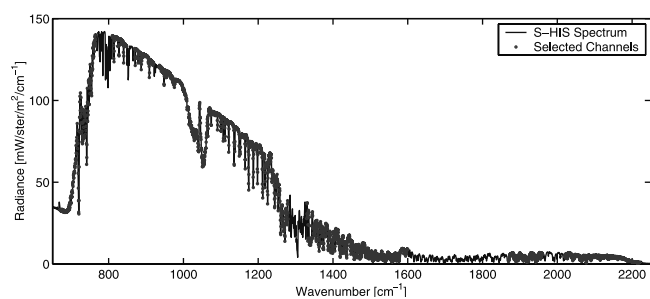
Figure 1. This sample full SHIS spectrum from 7 September 2000 shows the locations of channels used for the retrieval of atmospheric temperature and moisture profiles as well as surface temperature. The spectral region used for the CO retrieval appears at the right end centered near 2142 cm^{-1}.

as well as identification and retrieval of atmospheric abundances of various trace gases including column CO. Furthermore, the wide spectral coverage permits retrievals of surface temperature and spectrally varying surface emissivity and cloud properties. Internal calibration is obtained using two onboard UWis built blackbodies, one at ambient conditions, the other heated [*Moeller et al.*, 2003].

[11] Due to the oversampling of the nadir-only views on the 7 September 2000 flight and viewing the onboard calibration blackbodies after every 24 Earth views, most CO retrievals were performed using averages of 12 individual nadir views. The ER-2 ascent, descent, and turns were omitted from this data set, yielding 1020 average spectra from the total of 22,225 from the flight. Of these 1020 average spectra, 742 were determined to be largely cloud-free based on the lack of correlation between cold IR microwindow brightness temperatures in the 800–900 cm^{-1} region, which would indicate cold clouds, and evidence of a solar reflection spectrum in the 2000–3000 cm^{-1} region, which would indicate either bare soil or white clouds. As Figure 3 illustrates, most of the flight was free of visible clouds. CO retrievals of cloudy spectra tend to produce unusually low values due to the clouds blocking the view of the lower atmosphere where most of the CO typically resides. As discussed later, some residual cloudiness could contaminate a portion of these 742 FOVs. For detailed views of the Timbavati fire, CO retrievals were performed for individual FOVs.

3. Temperature and Water Vapor Retrievals

[12] The CO retrieval technique requires knowledge of the atmospheric temperature and water vapor vertical profile below the aircraft. Temperature and water vapor profiles were retrieved from the SHIS observations using the spectral regions indicated in Figure 1. The retrieval technique used is based on a linear regression applied according to the following procedure.

[13] A training set was constructed from 10,000 radiosonde profiles (air temperature, water vapor mixing ratio, surface pressure, and surface temperature) for the months of July–October between years 1990 and 1999. A forward model was used to generate 10,000 noise-free spectra of synthetic radiances at aircraft altitude from the radiosonde

data set. A principal component analysis reduced the dimensionality of the training data set from a large number of interdependent variables [*Huang and Antonelli*, 2001]. This reduction is achieved by finding a set of N orthogonal vectors in the input space of dimension M, with N smaller than M, which accounts for as much of the data variance as possible. The reduced radiance data set is then used with the radiosonde data set to determine a set of regression coefficients. These regression coefficients are used to map the radiance observations, properly reduced, to temperature and water vapor vertical profiles.

4. CO Retrieval Algorithm

[14] CO retrievals from SHIS spectra were performed using an algorithm previously demonstrated on HIS spectra by *McMillan et al.* [1996, 1997]. In this algorithm, the roughly regular spacing of the CO spectral lines in the 1-0 vibration-rotation band is exploited by a Fourier signal processing technique to retrieve the total column density of CO below the ER-2 [*Strow et al.*, 1993; *McMillan et al.*, 1996, 1997]. Column CO retrieval proceeds by varying a constant tropospheric (100 mb to surface) CO mixing ratio to minimize the residuals in the CO portion of the spectrum [*McMillan et al.*, 1997]. Forward model radiance calculations are performed with kCARTA [*DeSouza-Machado et al.*, 1997; *Strow et al.*, 1998] using the retrieved atmospheric profiles of temperature and water vapor as well as surface skin temperature and then convolved to SHIS resolution. Extensive sensitivity testing indicates total column CO can be retrieved to an accuracy of ~10% under most conditions [*McMillan et al.*, 1997].

[15] Major advantages of this algorithm are relative insensitivities to noise and uncertainties in water vapor. A major drawback of this algorithm is its reliance on an a priori shape for the CO profile. Although CO is not typically well mixed throughout the troposphere, it is often well mixed in the midtroposphere where the SHIS CO sensitivity function peaks. Using the technique of *McMillan et al.* [1997], the nominal SHIS CO sensitivity functions were calculated as shown in Figure 2. Nearly identical spectral resolutions between HIS and SHIS make these functions virtually the same. Although the sensitivity decreases near the surface due to decreasing thermal contrast between the atmosphere and surface, the sensitivity to boundary layer CO is not negligible.

[16] This sensitivity to the boundary layer enables SHIS to see CO enhancements due to forest fires [*McMillan et al.*, 1996] and should make it possible to detect regions of urban pollution. Unfortunately, errors in SHIS retrieved column CO up to ~25% can be expected where the boundary layer is most polluted [*McMillan et al.*, 1997]. However, *McMillan et al.* [1996] demonstrate boundary layer enhancements due to biomass burning plumes are observed readily by remote sensing thermal emission spectra. This technique for CO remote sensing in the vicinity of fires is significantly different from that used by *Stearns et al.* [1986] in which the hot fire itself was used as a source.

[17] As further demonstrated by *McMillan et al.* [1996], significant information on the magnitude of boundary layer CO enhancements can be obtained from the SHIS spectra when the CO retrieval algorithm is modified with ancillary
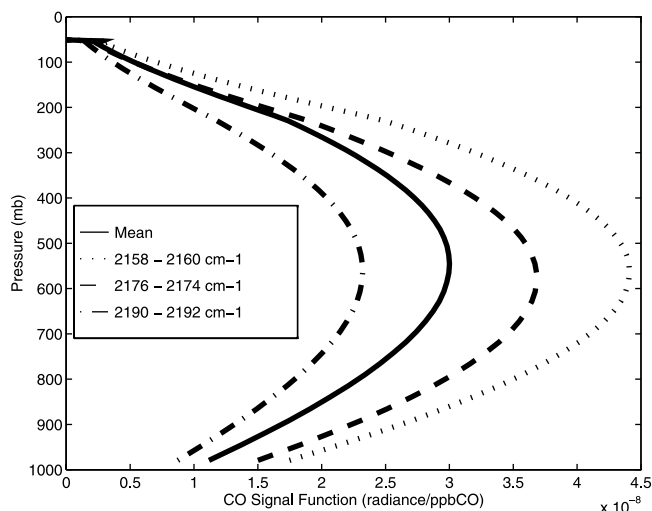
Figure 2. CO sensitivity functions (SF_{CO}) for a constant CO mixing ratio in the troposphere, AFGL standard atmosphere, and surface air thermal contrast of 5 K. SF_{CO} for CO lines at 2158.2997, 2176.284, and 2190.018 cm^{-1} are shown along with the mean SF_{CO} for the 17 CO lines in the 2135–2200 cm^{-1} spectral region. SF_{CO} were calculated for the nearest SHIS frequencies using the method of *McMillan et al.* [1997].

information such as knowing where in the atmosphere CO enhancements are confined. CO retrievals can be performed by setting any portions of the CO profile at a fixed value and varying any other pressure layers [*McMillan et al.,* 1996]. In the present work, no such attempt has been made to separate boundary layer and mean free tropospheric CO abundances. Rather, the comparisons of changes in the retrieved constant tropospheric CO mixing ratios from SHIS spectra to the available in situ observations clearly indicate the sensitivity of the SHIS CO retrievals to boundary layer CO enhancements.

5. 7 September 2000 Flight

[18] The flight of 7 September 2000 took the ER-2 over a widely varying atmosphere including a controlled burn near Kruger National Park in northeastern South Africa with generally clean continental air in the vicinity, clean marine air over and southeast of Inhaca Island off the southeastern coast of Mozambique, and biomass smoke laden air just at the edge of the dying *river of smoke* over south central Mozambique. The ER-2 flight track is overlaid on a Meteosat visible image in Figure 3. The controlled burn occurred in the Timbavati Game Reserve bordering Kruger National Park and hereafter will be referred to as the Timbavati fire. The *river of smoke* feature widely reported in NASA press releases as imaged by the SeaWIFS satellite and indicated by retrievals of atmospheric aerosol indices (AI) from TOMS is discussed in more detail by Annegarn et al., (submitted manuscript, 2003). TOMS aerosol maps are discussed further below.

[19] Two other aircraft participating in SAFARI 2000 also flew in the vicinity of the Timbavati fire on 7 September 2000: the University of Washington Convair-

580 (CV) and a South African Aerocommander (JRB). Both aircraft made a number of in situ measurements of trace gases and aerosol properties as described in detail in other papers in this issue (see Appendix A by P. V. Hobbs in the work of *Sinha et al.* [2003]) [*Hobbs et al.,* 2003; *Sinha et al.,* 2003; S. Piketh et al., An overview of in situ airborne measurements onboard the South African Aerocommanders JRA and JRB during SAFARI-2000, submitted to *Journal of Geophysical Research,* 2003, hereinafter referred to as Piketh et al., submitted manuscript, 2003.]. Another South African Aerocommander aircraft (JRA) crossed paths with the ER-2 over Inhaca Island, southern Mozambique, and northeastern South Africa (Piketh et al., submitted manuscript, 2003). Comparisons between CO measurements made by these aircraft and SHIS CO retrievals are presented in a following section.

5.1. Meteorology

[20] One of the dominating features of southeastern African meteorology on 7 September 2000 is evident in the Meteosat image (Figure 3) as the band of clouds off the east coast of South Africa and southern Mozambique. These clouds were associated with a weakening baroclinic westerly wave (weather front) moving to the northeast. Such westerly waves produce most of the mixing in the southern African atmosphere during the winter and sweep biomass burning products from central Africa out over the Indian Ocean [*Freiman et al.,* 2002] as in the *river of smoke* (Annegarn et al., submitted manuscript, 2003). The day of 7 September 2000 marked a transition between the westerly wave conditions that led to the *river of smoke* flow over the Indian Ocean and the more typical large-scale subsidence in the anticyclonic continental high conditions of the southern African gyre [*Freiman et al.,* 2002].

5.2. TOMS AI

[21] The *river of smoke* event was quite evident in plots of the AI as retrieved from observations by TOMS. The particulars of TOMS AI retrievals are given by *Herman et al.* [1997] and *Torres et al.* [1998]. Figure 4 shows the TOMS AI over a portion of the Southern Hemisphere centered on Africa for 7 September 2000. The waning *river of smoke* is just visible as the higher values off the east coast of Africa between Mozambique and Madagascar and in a thin plume stretching to the southeast over the Indian Ocean. Thus, the TOMS AI serves as a tracer for the previously discussed large-scale meteorological transport.

5.3. Back-Trajectories

[22] Overlaid on the TOMS AI map of Figure 4 are trajectories representative of passive tracer transport for particles with final destinations located along a portion of the ER-2 flight track. Back-trajectories initialized at the measurement locations were calculated with the Goddard Space Flight Center trajectory code using the UK Meteorological Office (UKMO) initialization fields. Here, back-trajectories for particles located at 26.42°S, 33.02°E and 25.01°S, 34.32°E at an altitude of 800 mb, and at time $t = $ 0800 UTC for 7 September 2000 are integrated for 5 days with particle positions stored every 12 hours. Qualitatively similar trajectories are produced for particles initiated at the same location and altitude but at 1200 UTC on 7 September
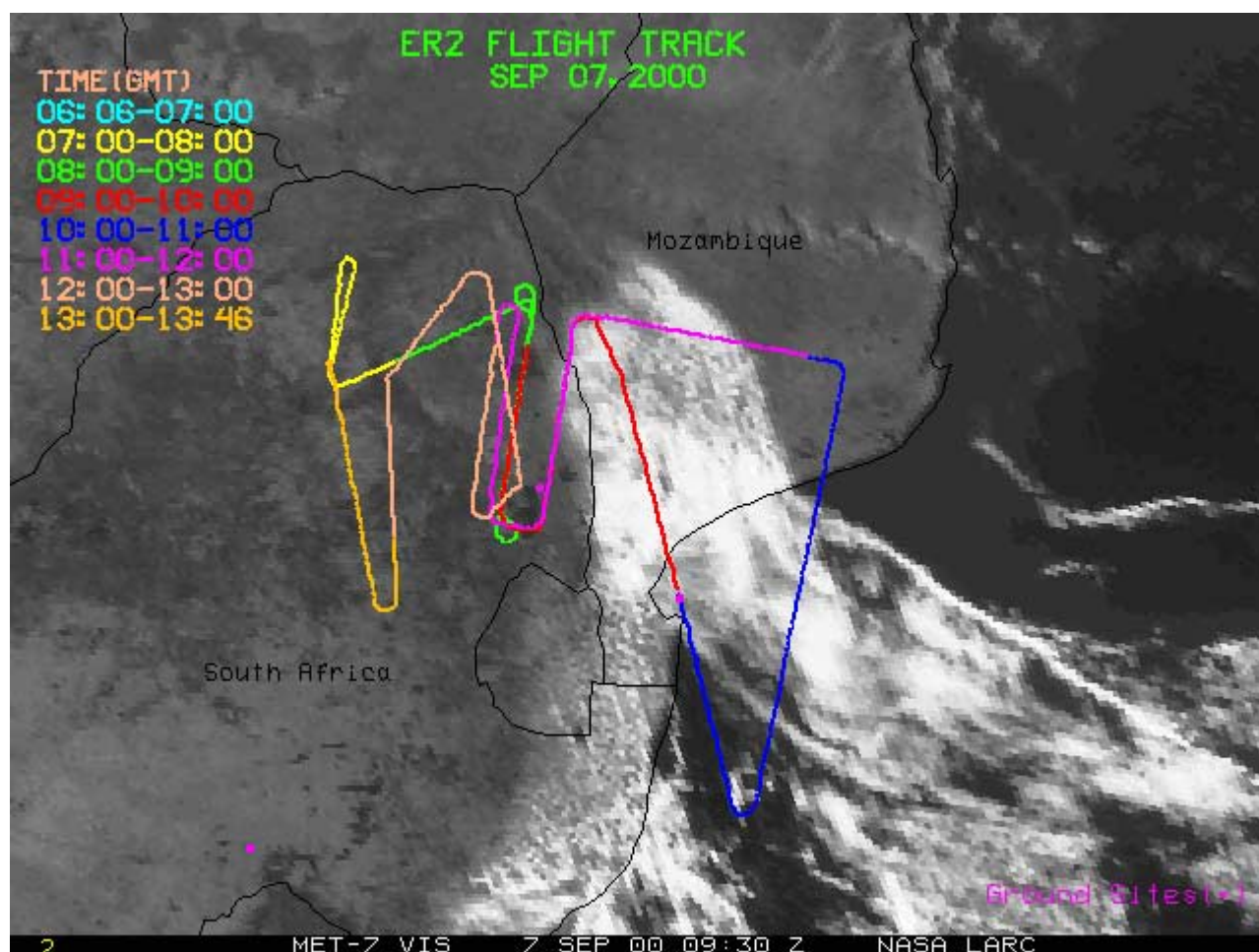
Figure 3. The ER-2 flight track for 7 September 2000 with different portions of the flight in different colors is overlaid on a Meteosat visible image taken at 0930 UTC the same day. The *river of smoke* lies to the north and east of the prominent cloud band stretching from southern Mozambique to the southeast corner of the image (image courtesy of NASA LaRC).

2000. It should be noted that although back-trajectories indicate the nature of large-scale transport in the present case thus providing a sense of the source region, some uncertainty exists in calculation of the trajectories due to the temporal resolution of the winds. In addition, integrations for the ensemble of particles comprising the clusters located to the east (red trajectory) and west (green trajectory) of the front demonstrate a divergence in trajectories over the source region with time. Moreover, there is uncertainty associated with particle advection at 800 mb due to its proximity to the boundary layer. The results are, however, qualitatively consistent with those found from column ozone measurements and TOMS data.

[23] The red ensemble is for points ahead of the front and indicates descent from 500 mb starting at the 5-day back point. Although the divergence of the trajectories increases backward in time, the entire ensemble shows recirculation and subsidence in the southern African gyre. The general descent of these trajectories is consistent with the dominance of a continental high before passage of the westerly wave. Below 800 mb, winds at cloud level derived from Meteosat images and the flow evident in the daily TOMS AI

maps show prevailing transport from the northwest to southeast.

[24] The green ensemble started for points just behind the front and indicates lifting from 950 to 800 mb along the path. The spread in this ensemble is much greater 5 days back, but the entire ensemble indicates a source region over the much cleaner south Atlantic. Below 800 mb, winds at cloud level derived from Meteosat images show low-level transport from the south and east bringing in clean marine air behind the front.

6. SHIS CO Retrievals

[25] Figure 5 presents tropospheric column CO retrievals along the full flight path of the ER-2 overlaid on top of the TOMS AI map. These retrievals were performed on averages of 12 spectra with all ER-2 aircraft turns and cloudy scenes removed. In addition, the largest CO columns from the Timbavati fire (center of white circle on map) were omitted to alter the CO color scale, thus enhancing the visibility of the smaller variations in column CO elsewhere along the flight track. CO retrievals along
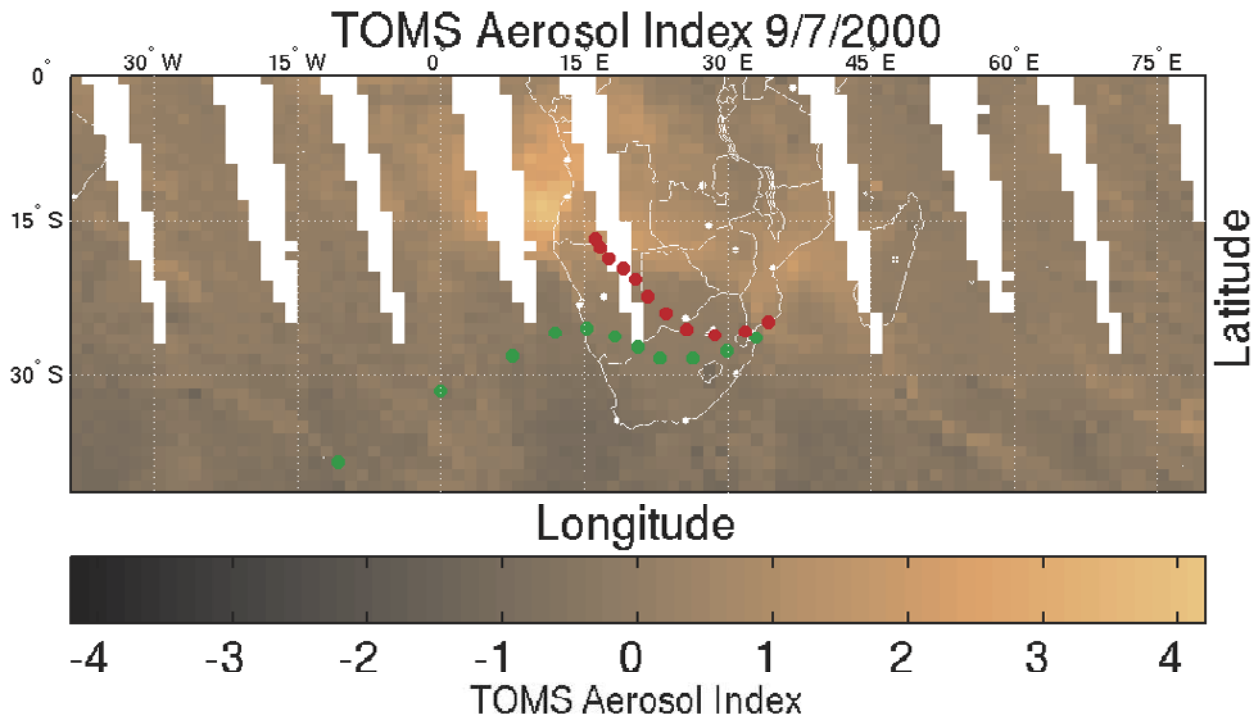
Figure 4. TOMS aerosol indices are mapped for a portion of the Southern Hemisphere for 7 September 2000 showing the dying *river of smoke* extending into the Indian Ocean from Mozambique to Madagascar and southeast. The two dotted lines show representative 5-day back-trajectories with marks every 12 hours for parcels started in the vicinity of ER-2 observations over Inhaca Island off the far southern coast of Mozambique (green circles) and south central Mozambique (red circles).

the Timbavati fire transects are discussed in more detail below.

[26] The Timbavati fire retrievals are included in the top panel of Figure 6 along with the retrievals from the previous map in Figure 5. The bottom panel of Figure 6 illustrates the expected variation in tropospheric CO column due to topographic and aircraft flight altitude variations alone. The pronounced differences between these two plots indicate real atmospheric variation in tropospheric column CO. The FOVs nearest the fires are clearly evident between 8.0 and 9.25 UTC as are the differences southeast of Inhaca Island (10.0 and 10.5 UTC) and south central Mozambique (10.75–11.25 UTC). For ease of plotting and comparison between the seven different data sets, all times are given in decimal hours. The larger scatter evident in the retrievals over the ocean southeast of Inhaca Island could result from residual cloud contamination of some of the averaged spectra. However, the lower values could reflect cleaner air further offshore.

6.1. River of Smoke

[27] Most obvious in Figure 5 is the correlation between retrieved CO column and TOMS AI with the largest values of both occurring over southeastern Mozambique. This is precisely the location of the southern edge of the waning *river of smoke*. The red back-trajectory ensemble previously discussed in Figure 4 was launched from the locations of these enhanced CO values. Thus, these large CO values are correlated with the transport out of Africa of biomass

burning products from central Africa formerly caught up in the southern Africa gyre.

[28] The second set of trajectories, green ensemble from Figure 4, were launched from the locations of the CO retrievals off the far southeast coast of Mozambique in the vicinity of Inhaca Island (white X in Figure 5). The smallest values of CO retrieved for this flight occurred in this area consistent with the trajectory and cloud wind transport of cleaner marine air. Aiding this comparison of the two air masses on either side of the frontal system is the fact that this entire section of the flight occurred over the ocean or low lying coastal regions as reflected in the lower panel of Figure 6. This variation of tropospheric CO on either side of a frontal system resulting from transport from widely differing source regions is reminiscent of the findings of *Doddridge et al.* [1998], *McMillan et al.* [1997], and *Connors et al.* [1989].

6.2. Timbavati Fire

[29] Figure 6 shows the enhanced CO columns retrieved along the three flight segments over the Timbavati fire between 8.0 and 9.25 UTC. The first and third segments were flown in the same direction and directly overlay each other; the second segment was slightly offset. Due to this offset, only the first and third segments will be discussed in detail here.

[30] CO retrievals from the averages of 12 spectra along the full length of the first and third Timbavati fire tracks are shown in the bottom panel of Figure 7 along with surface
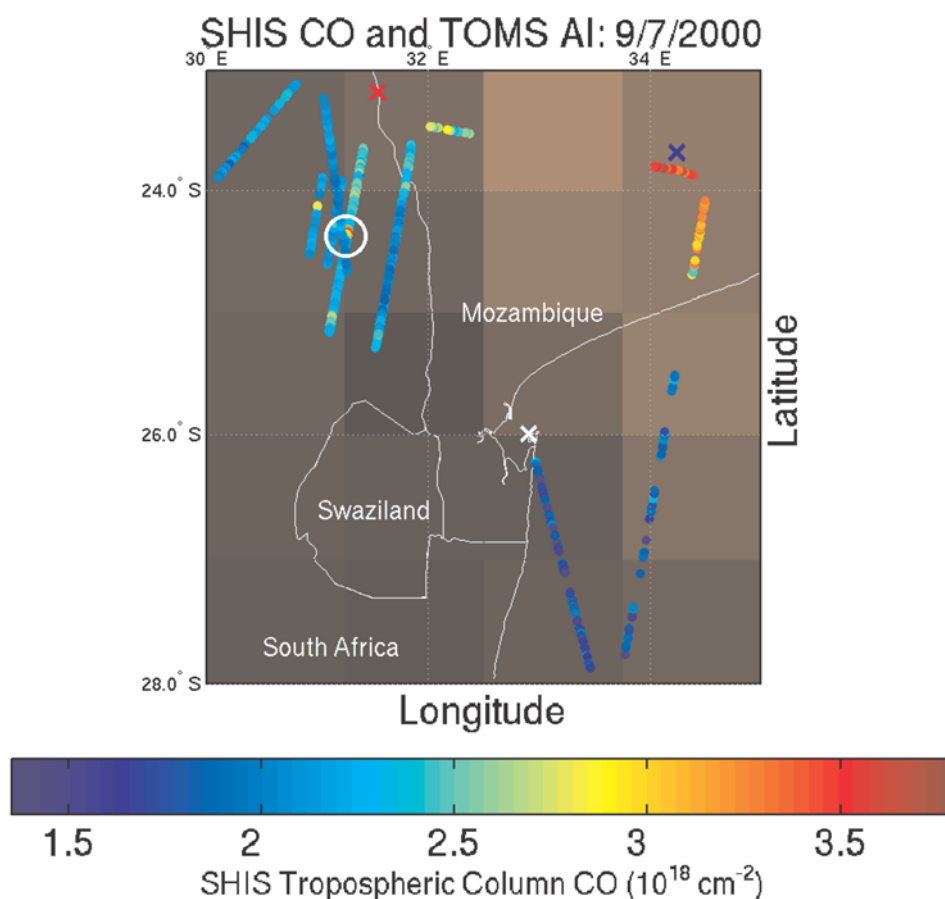
Figure 5. SHIS retrievals of tropospheric column CO for 742 averages of 12 spectra are overlaid in the colored circles on the TOMS AI map. The color scale for TOMS AI corresponds to that used in the full TOMS AI image of Figure 4. The location of the Timbavati fire lies at the center of the large white circle in the upper left of the image. Note the two larger CO columns at the fire. Locations of the three in situ CO profiles from the JRA aircraft are noted by the colored X's. White denotes Inhaca Island, blue south central Mozambique, and red northeastern South Africa.

temperatures retrieved from SHIS spectra in the top panel. Evident in the surface temperature retrievals are 10 K variations due to different surfaces such as the lower values at times 8.26 and 8.29 UTC when the ER-2 overflew old burn scars. Note the warming of the surface apparent between the nearly coincident flight tracks approximately 0.75 hours (44 min) apart. Although there is some impact of the varying surface temperatures on the CO retrievals in the lower panel, the largest impact on retrieved CO is evident in the center of the two tracks: the Timbavati fire.

[31] The retrieved surface temperatures indicate the nadir looking SHIS FOV may have largely missed the actual fire itself but observed the plume of burning products at 8.36 UTC. The slight increase in retrieved surface temperature around 8.355 may be due to smoldering on a recent burn scar from the previous day or due to the burn scar itself. The enhanced CO retrieved in this area points to smoldering as the more likely cause.

[32] While all of the largest retrieved CO columns do not coincide with increases in retrieved surface temperature, they do coincide with a substantial increase in scattering of sunlight from the smoke plume back to SHIS as evident in

the short-wave portions of some spectra. Although the solar radiance spectrum decreases toward longer wavelengths, solar scattering from the dense smoke plume is not negligible in the portion of the spectrum used for CO retrievals. A first-order correction for scattered sunlight was applied for CO retrievals over the smoke plume by retrieving an effective surface temperature directly from the relatively transparent center of the CO 1-0 vibration-rotation band near 2142 cm^{-1}. As a result of this correction, the CO retrievals over the thickest portions of the smoke plume are more uncertain than those in clear air and likely represent upper limits. A more detailed radiative transfer calculation for the case of solar scattering in smoke plumes is the subject of ongoing research.

[33] To examine the detailed spatial extent of CO near the Timbavati fire, CO retrievals were performed for 144 individual SHIS spectra from each of the first and third fire tracks centered on the fire. These retrievals are depicted in Figure 8 along with the retrievals from the averages of 12 spectra. This figure shows the CO retrievals from averaged spectra are nearly identical to the average CO retrieved from the corresponding 12 individual spectra. With these two
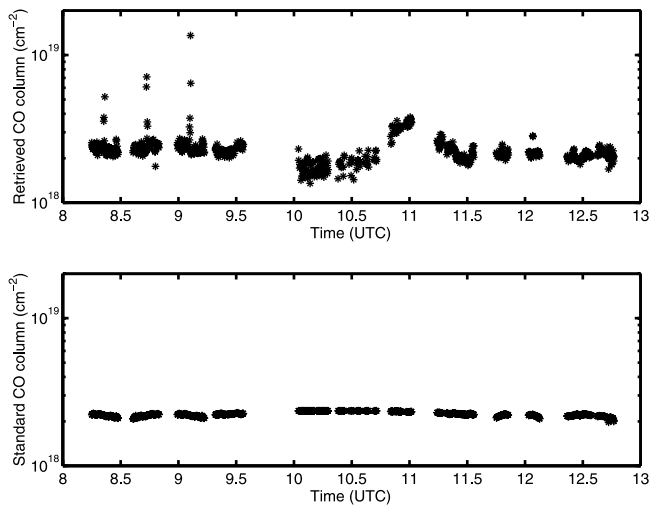
Figure 6. The top panel depicts retrievals of total tropospheric column CO from 742 cloud-free averages of 12 SHIS spectra acquired on 7 September 2000 during SAFARI 2000. The bottom panel shows the expected spatial variation in total tropospheric CO column due to topographic and aircraft flight altitude variations. The dissimilarity between these two plots implies substantial real variations in tropospheric column CO.

flight tracks nearly coincident, we can look for temporal changes in the spatial extent of the CO sources with the caveat that calibration gaps appear at different locations in the two tracks.

[34] The CO smoldering region around 8.355 UTC appears roughly identical between the two tracks with nearly the same magnitude and spatial extent. The third track has a calibration gap exactly at the location of the central dip seen in the first track at 8.355 UTC.

[35] The larger peak over the smoke plume shows changes in location (shape) and magnitude. Although a calibration gap in the first pass misses most of the peak column CO seen in the third pass, both tracks have data at the location of 8.36 UTC. Here, the first track shows near background values while the third track is nearly 10 times larger. However, between 8.363 and 8.364 UTC, the first pass shows higher values than the third pass. These variations imply either changes in fire or smoke plume location along the track or changes in fire intensity. Given that the fire was started shortly before the ER-2 overpass, it is likely the CO levels increased with time as the fire grew. Changes in the spatial extent of the CO enhancement could be due to fire growth as well as slight changes in local wind direction.

7. In Situ CO Measurements

[36] Two other aircraft participating in SAFARI 2000 flew in the vicinity of the Timbavati fire on 7 September 2000 and one other aircraft crossed paths with the ER-2 over other portions of its flight. Details of the investigations performed by the University of Washington Convair-580 (CV) research aircraft during SAFARI 2000 and in the vicinity of the Timbavati fire are described elsewhere in this issue (see Appendix A by P. V. Hobbs in the work of *Sinha et al.* [2003]) [*Hobbs et al.*, 2003; *Sinha et al.*, 2003].

Other activities of the South African Aerocommander aircraft, JRA and JRB, are described elsewhere in this issue (Piketh et al., submitted manuscript, 2003). JRB performed vertical profiling in the vicinity of the Timbavati fire, while JRA executed profiles over Inhaca Island off the far southern coast of Mozambique, over south central Mozambique, and on the return to Pietersburg. A brief description of the CO measurements made by each of these aircraft is provided below with citations to more complete references.

7.1. CV

[37] Three systems were operating onboard the CV measuring CO: a Thermo Environmental Instruments model 48 CO gas analyzer (TECO 48), canister samples analyzed by gas chromatography (GC), and in situ measurements with an AFTIR spectrometer (see Appendix A by P. V. Hobbs in the work of *Sinha et al.* [2003]). Vertical profiles were obtained both inside and outside the Timbavati smoke plume as well as transects across the smoke plume at various distances downwind [*Hobbs et al.*, 2003; *Sinha et al.*, 2003]. Measurements onboard the CV were obtained from 8.5 to 10.5 UTC with approximately one third of these collected during the times of the three ER-2 overpasses of the Timbavati fire region.

7.1.1. TECO 48

[38] An unmodified TECO 48 generally provided more continuous measurements, but the only TECO 48 data presented here are for samples taken in the smoke plume. This is because the TECO 48 was calibrated for maximum sensitivity in the range of the high concentrations expected and encountered in the smoke plume with a precision of ±21% (see Appendix A by P. V. Hobbs in the work of *Sinha*
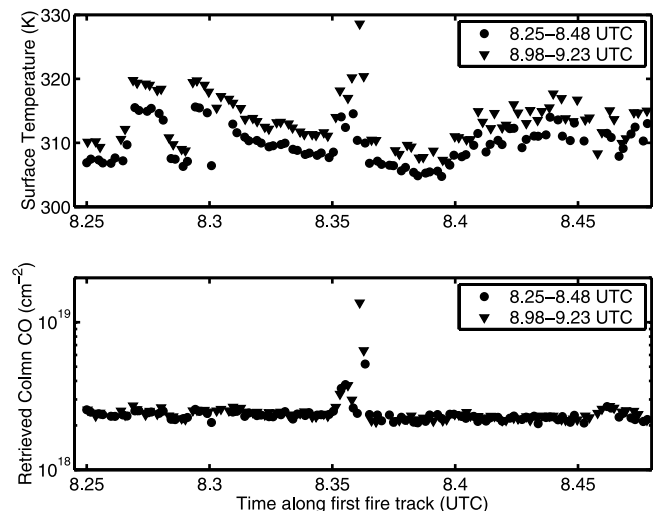

Figure 7. The top panel shows the surface skin temperatures retrieved from thermal window channels in averages of 12 SHIS spectra along the first and third ER-2 tracks over the Timbavati fire. The lower panel presents the total tropospheric CO columns retrieved from the same averages of 12 SHIS spectra. Due to the near coincidence of these two tracks, they have been overlaid on the same x axis scale to show intertrack variations. The locations of the third track (8.98–9.23 UTC) were interpolated to the times of the first track (8.25–8.48 UTC).
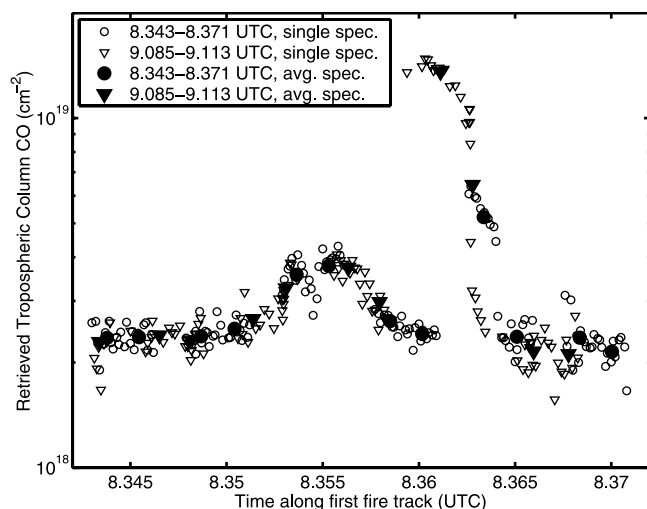
Figure 8. Tropospheric CO columns retrieved from 144 individual SHIS spectra along each of the first and third fire tracks over the Timbavati fire are shown. There is general agreement of the retrievals along the two tracks, including the bump centered at 8.355 UTC. However, the detailed shape of the maximum retrieved CO columns closest to the active fire (8.36–8.364 UTC) differs substantially between the two overpasses. Also plotted are the corresponding CO columns retrieved from the averages of 12 SHIS spectra along the same tracks. The values from the averages are also shown in the central portion of Figure 7. As in that figure, the SHIS FOV locations along the third ER-2 fire track were interpolated to the times of the first track so the observations from these two spatially coincident tracks could be overlaid to illustrate intertrack variations.

et al. [2003]). Thus, only the four data points taken in the smoke plume are presented for comparison with the other techniques.

7.1.2. GC

[39] Using a stainless steel inlet passed through the fuselage of the CV, electropolished stainless steel canisters were filled with sample air from smoke plumes and from background air just upwind of the fires (Hobbs, submitted manuscript, 2003). These samples were later analyzed with different techniques for different gases including GC for CO with a precision of 10% [Hobbs et al., 2003; Coleman et al., 2001]. Four GC measurements are presented here, each obtained at the same times and locations as the four CV TECO 48 measurements.

7.1.3. AFTIR

[40] In situ CO measurements were made with the Airborne FTIR instrument (AFTIR) [Yokelson et al., 1999, 2003] onboard the CV in background air near the fire and at various locations in the smoke plume up to 28 km downwind from the fire. The AFTIR inlet directed ram air through a Pyrex multipass cell with an exchange time of 4–5 s. AFTIR acquired the infrared spectrum of the cell contents every 0.83 s at 0.5 cm^{-1} resolution. In addition, the inlet and outlet valves of the cell could be closed to detain whole air samples for 2–3 min of signal averaging which allowed improved measurements of CO and the other major reactive and stable trace gases present above 5–20 ppbv.

The AFTIR CO retrievals were based on a large number of calibration spectra of dynamically prepared flowing standards recorded both before and after the research flights. This calibration yields a measured precision of 0.6%, 0.9 ppb at nominal background levels, and an estimated accuracy of 1–2%. A complete description of the AFTIR system and typical CO vertical profiles for the southern African dry season are provided by *Yokelson et al.* [2003].

7.2. JRB

[41] The South African Aerocommander aircraft JRB, flew with two systems for CO measurements: a modified TECO 48 C and a NOAA CMDL flask sampling suitcase (Piketh et al., submitted manuscript, 2003). To provide in situ validation for MOPITT with an overpass near the Timbavati fire, JRB performed a vertical profile from approximately 350 to 950 mb from 7.75 to 9.1 UTC overlapping the times of the three ER-2 overpasses.

7.2.1. CMDL Flasks

[42] The widely accepted standard for in situ CO measurements provided by the CMDL flask sampling system and the requisite measurement protocols are described by *Novelli et al.* [1992, 1994], *Lang et al.* [1992], and *Conway et al.* [1994]. For the 7 September 2000 flight, 20 samples were collected with 19 high quality measurements made with a nominal precision in CO mixing ratio of ~1% [*Novelli et al.*, 1998a]. However, the large values found in the smoke plume are well above the range of the reference gases used for the analysis, and thus, are more uncertain. These CO measurements are referenced to the revised CMDL99 (P. C. Novelli et al., Effects of the 1997/1998 wildfires on global CO distributions and long-term trends, submitted to *Journal of Geophysical Research*, 2003).

7.2.2. TECO 48 C

[43] Aboard the JRB was a high-performance modified TECO 48 C for enhanced sensitivity following the methods of *Dickerson and Delany* [1988] as widely used for other in situ measurements [*Doddridge et al.*, 1994, 1998]. This instrument has a detection limit of ~24 ppbv for a 1 min mean of 10 s data and was calibrated premission and postmission against a ~2 ppmv working standard of CO which, in turn, is referenced regularly to a National Institute of Standards and Technology (NIST)/Standard Reference Material. The JRB CO data reported here were renormalized relative to the NOAA/CMDL scale [*Novelli et al.*, 1998b] based upon laboratory calibrations performed after SAFARI 2000 against three CMDL standards of 50, 200, and 350 ppbv. Under the field experimental conditions applicable for SAFARI 2000, the TECO 48 C measurements are not reliable at pressures <670 mb.

7.3. JRA

[44] The South African Aerocommander aircraft JRA, flew with one system for CO measurements: a stock TECO 48C-TL (Piketh et al., submitted manuscript, 2003). The data shown here are for three profiles with locations noted in Figure 5: over Inhaca Island off the far southern coast of Mozambique, over south central Mozambique, and on the return flight to Pietersburg. Due to the lack of exact temporal and spatial coincidence between the JRA and the ER-2 on this day, we only present this as a very qualitative comparison. The JRA completed the Inhaca Island profile
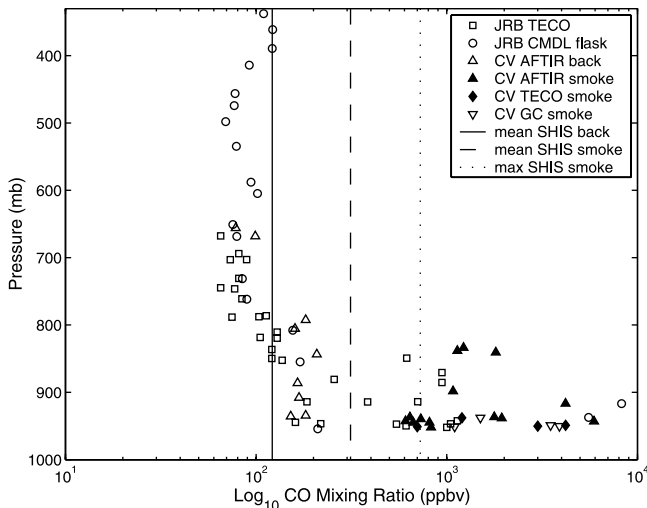
Figure 9. A comparison of all the available in situ and remote sensing measurements of CO in the vicinity of the Timbavati fire is presented. Note the good agreement between JRB TECO, JRB CMDL flask, and AFTIR measurements in background air, pressures < 850 mb and near the AFTIR open triangles for pressures >850 mb. The larger CO values occurred in the smoke plume and illustrate the temporal and spatial variability of the fire and resultant smoke.

approximately 30 min before the ER-2 overpass; it was still 30 min ahead of the ER-2 over south central Mozambique, but it was more than 2 hours behind the ER-2 for the return leg to Pietersburg.

8. Timbavati Fire Comparison

[45] Figure 9 illustrates the full comparison of all available CO data for the vicinity of the Timbavati fire on 7 September 2000. SHIS CO retrievals are given in terms of the constant tropospheric CO mixing ratio for ease of comparison to the in situ data. Table 1 presents a comparison of the SHIS column CO retrievals to those calculated for composite CMDL flask + AFTIR measurements in the background and smoke plume.

[46] As shown in Figure 9, all of the various in situ CO measurements are in qualitative agreement. In particular, note the good agreement between the JRB TECO, and CMDL flask samples and the AFTIR for regions not affected by the smoke plume, pressures <800 mb and near the AFTIR background values for pressures >850 mb. In the smoke plume, the various in situ measurements are highly variable due to the spatial and temporal variability of the fire and smoke [see *Hobbs et al.*, 2003, Figure 1], the different locations of the measurements in time and space, and the different response times of the five in situ instruments. Thus, the values plotted illustrate the range of variability but may not even capture the true local maximum. While the observed 0.6–8 ppmv values are substantially enhanced over background values, they lie well within the 1.2–15 ppmv range found by previous airborne investigations in biomass smoke plumes [*Kaufman et al.*, 1992; *Harriss et al.*, 1994; *Goode et al.*, 2000].

[47] Representing retrievals of tropospheric column CO with the constant tropospheric CO mixing ratio, it is difficult to compare readily the SHIS CO retrievals to in situ measurements. However, we can clearly state the SHIS CO retrievals follow the background-to-plume variation in CO seen in the in situ measurements. In addition, we can state conclusively that the SHIS CO retrievals are sensitive to boundary layer CO in confirmation of previous results [*McMillan et al.*, 1996]. Comparisons of actual CO columns are more meaningful as provided in Table 1.

[48] All CO columns reported in Table 1 were computed for a total tropospheric column from the surface (~400 m) to a nominal tropopause at 100 mb, thus necessitating some means of extrapolation for the CMDL profile which started at 337 mb. Given the relatively constant CO mixing ratio measured by the CMDL flask samples in the free troposphere, a constant CO mixing ratio equal to the mean free tropospheric value (91 ppbv) was assumed from 337 mb to 100 mb. With the similarity between the JRB TECO, CMDL, and AFTIR values shown in Figure 9 above the smoke plume, p < 800 mb, and in the relatively cleaner portions of the boundary layer outside of the smoke plume (<200 ppbv), a background CO profile was constructed by combining the AFTIR background measurements with the CMDL measurements excluding the two ppmv CMDL points that obviously lie within the smoke plume. To calculate the total tropospheric CO column including the smoke plume, all CMDL measurements were used with the same extrapolation for the top portion of the profile.

[49] The comparisons between SHIS retrieved tropospheric CO columns and the CMDL, CMDL + AFTIR measured columns are quite satisfying given the variable conditions near the fire. The mean SHIS retrieved background tropospheric CO column of 2.3×10^{18} cm^{-2} is only 9.5% higher than the measured/extrapolated CMDL profile of 2.1×10^{18} cm^{-2}. The sensitivity studies performed for CO retrievals from HIS indicate an expected accuracy no better than ~10% and perhaps up to 25% in conditions of polluted boundary layers [*McMillan et al.*, 1997]. Within the observed variations in SHIS background tropospheric CO columns of 0.25×10^{18} cm^{-2}, the SHIS and CMDL + AFTIR columns are identical statistically.

[50] In the case of the smoke plume itself, the maximum SHIS retrieved tropospheric CO column matches the total tropospheric CMDL measured/extrapolated profile. Given

Table 1. Quantitative Comparison of SHIS Retrieved Total Tropospheric Column CO and CMDL + AFTIR In Situ Measured/Extrapolated Total Tropospheric Column CO in the Vicinity of the Timbavati Fire for Both Background Air and Qualitatively for the Smoke Plume are Given[a]

Instrument	Background Column CO $\times$ 10^{18} cm^{-2}	Smoke Plume Column CO $\times$ 10^{18} cm^{-2}
CMDL		15
CMDL + AFTIR	2.1	
SHIS mean	2.3	4.6
SHIS 1σ	0.25	3.5
SHIS max	3.1	15
SHIS min	1.6	2.0

[a]The uncertainties listed for the SHIS background columns represent the 1σ variations in 132 retrieved background columns near the fire and for the 36 SHIS spectra most impacted by the fire and smoke.
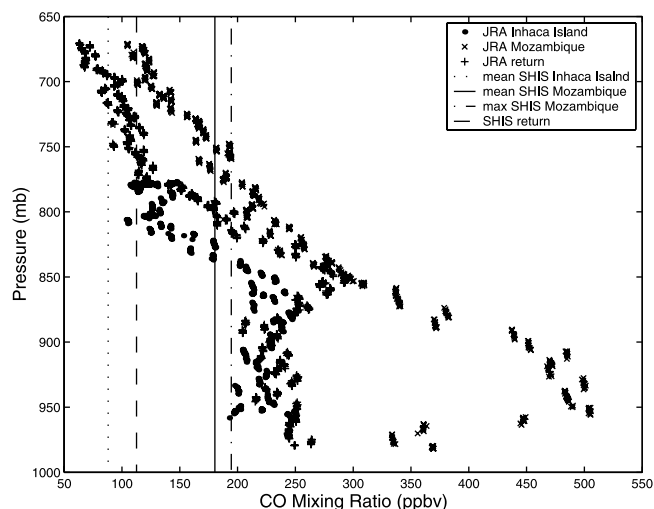
Figure 10. The comparison of JRA CO in situ CO profiles and SHIS CO retrievals presented here is for qualitative purposes. Note the larger CO values seen by JRA at all levels over the *river of smoke* in Mozambique (X's) as compared to the two profiles acquired on the other side of the westerly wave. The SHIS retrievals show the same spatial variations.

the temporal and spatial variations evident in both the SHIS retrievals and the in situ measurements, this result is partly fortuitous. With the multisecond response times of the in situ instruments, it is possible none of the measurements sampled the true maximum amount of CO present in the plume. Moreover, it is unlikely the 2 km size of the SHIS FOV was filled with a uniform scene of the smoke plume containing no background scenes. However, the nearly constant retrieved CO columns from eight consecutive SHIS spectra at the peak of the third pass (near 8.36 UTC) indicate the presence of an extended source. MAS data could enable detailed modeling of SHIS FOVs for both cloudy [*Wang et al.*, 2000] and fire scenes; however, this goes beyond the scope of the present investigation. A highly variable and underresolved active fire and smoke plume is not the target of choice for carrying out a validation exercise, but the results here clearly demonstrate the sensitivity of SHIS to boundary layer CO.

9. SHIS and JRA Comparison

[51] Comparisons between the in situ measurements on JRA and SHIS constant tropospheric CO mixing ratio retrievals are presented in Figure 10. Again, these are provided for qualitative comparison only. The lack of adequate temporal and spatial coincidence makes a quantitative comparison problematic. As for the quick comparison of the Timbavati measurements and retrievals, we see that generally SHIS detected the larger CO values measured in situ.

[52] As previously discussed with regard to Figure 5, the SHIS retrievals display sensitivity to the CO enhancements found in the *river of smoke* over south central Mozambique. However, the JRA profile indicates this CO enhancement was not totally confined to the boundary layer, but extended to the top of the measured profile when compared to the JRA return profile over northern South Africa. The mean SHIS retrievals

of CO mixing ratio mimic the variation in the partial column measured by JRA with a progression of CO columns from the cleanest over Inhaca Island to more polluted over northern South Africa to most polluted over south central Mozambique. The smaller CO values found by SHIS southeast of Inhaca Island could reflect cleaner marine air further offshore than the JRA profile or result from retrieval inaccuracies due to partially cloudy averaged SHIS spectra.

10. Conclusions

[53] The results presented here demonstrate the utility and accuracy of remotely sensed tropospheric CO columns and abundances from AFTIR spectra. The capabilities of such high spectral resolution instruments for simultaneous retrievals of atmospheric conditions including trace gas abundances and surface/cloud properties is unparalleled. Existing (MOPITT and AIRS) and planned (TES and GIFTS) satellite instruments with similar capacities should enhance our ability to monitor atmospheric pollution.

[54] Comparison of remotely sensed and in situ total tropospheric CO columns (100 mb to the surface) agree well in the vicinity of the Timbavati fire observed on 7 September 2000. SHIS tropospheric CO column values of $(2.3 \pm 0.25) \times 10^{18}$ cm^{-2} over background air near the fire and $(1.5 \pm 0.35) \times 10^{19}$ cm^{-2} over the smoke plume agree extremely well with measured tropospheric CO columns extrapolated from 337 to 100 mb, of 2.1×10^{18} cm^{-2} in background air and up to 1.5×10^{19} cm^{-2} in the smoke plume. Qualitative comparisons with three other in situ CO profiles obtained over Mozambique and northern South Africa show the influence of the *river of smoke* and the capability of remotely sensed spectra to observe and measure such events.

[55] The remaining 13 SHIS flights from SAFARI 2000 await processing and detailed analysis with numerous additional opportunities for comparison between SHIS retrievals, in situ measurements, and the ARIES FTIR remote sensing instrument which flew on the UK C-130 aircraft [*Haywood et al.*, 2003; *Wilson et al.*, 1999]. Work on the data from these flights is progressing toward the development of a full suite of CO observations for validation of CO measurements made by MOPITT onboard the NASA Terra satellite.

References

Andreae, M. O., B. E. Anderson, D. R. Blake, J. D. Bradshaw, J. E. Collins, G. L. Gregory, G. W. Sachse, and M. C. Shipham, Influence of plumes

from biomass burning on atmospheric chemistry over the equatorial and tropical South Atlantic during CITE 3, *J. Geophys. Res.*, *99*, 12,793–12,808, 1994.

Annegarn, H. J., L. Otter, R. J. Swap, and R. J. Scholes, Southern Africa's ecosystem in a test tube: A perspective on the Southern African Regional Science Initiative SAFARI 2000, *S. Afr. J. Sci.*, *98*, 111–113, 2002.

Badr, O., and S. D. Probert, Carbon monoxide concentration in the Earth's atmosphere, *Appl. Energy*, *49*, 99–143, 1994.

Brunke, E. G., H. E. Scheel, and W. Seiler, Trends of tropospheric CO, N$_2$O, and CH$_4$ as observed at Cape Point, South Africa, *Atmos. Environ.*, *24A*, 585–595, 1990.

Chatfield, R. B., J. A. Vastano, H. B. Singh, and G. Sachse, A general model of how fire emissions and chemistry produce African/oceanic plumes (O$_3$, CO, PAN, smoke) in TRACE A, *J. Geophys. Res.*, *101*, 24,279–24,306, 1996.

Chatfield, R. B., J. A. Vastano, G. W. Sachse, and V. S. Connors, The great African plume from biomass burning: Generalizations from a three-dimensional study of TRACE A, *J. Geophys. Res.*, *103*, 28,059–28,077, 1998.

Christopher, S. A., J. Chou, and R. M. Welch, Satellite investigations of fire, smoke, and carbon monoxide during April 1994 MAPS mission: Case studies over tropical Asia, *J. Geophys. Res.*, *103*, 19,327–19,336, 1998.

Clerbaux, C., J. Hadji-Lazaro, D. Hauglustaine, G. Megie, B. Khattatov, and J. Lamarque, Assimilation of carbon monoxide measured from satellite in a three-dimensional chemistry-transport model, *J. Geophys. Res.*, *106*, 15,385–15,394, 2001.

Cofer, W. R., J. S. Levine, E. L. Winstead, D. R. Cahoon Jr., D. I. Sebacher, J. P. Pinto, and B. J. Stocks, Source compositions of trace gases released during African savanna fires, *J. Geophys. Res.*, *101*, 23,597–23,602, 1996.

Coleman, J. J., A. L. Swanson, S. Meinardi, B. C. Sive, D. R. Blake, and F. S. Rowland, Description of the analysis of a wide range of volatile organic compounds in whole air samples collected during PEM-T A and B, *Anal. Chem.*, *73*, 3723–3731, 2001.

Connors, V. S., T. Miles, and H. G. Reichle Jr., Large-scale transport of a CO-enhanced air mass from Europe to the Middle East, *J. Atmos. Chem.*, *9*, 479–496, 1989.

Connors, V. S., D. R. Cahoon Jr., H. G. Reichle Jr., and H. E. Scheel, Comparison between carbon monoxide measurements from spaceborne and airborne platforms, *Can. J. Phys.*, *69*, 1128–1137, 1991a.

Connors, V. S., D. R. Cahoon Jr., H. G. Reichle Jr., E. G. Brunke, M. Garstang, W. Seiler, and H. E. Scheel, Savanna burning and convective mixing in southern Africa: Implications for CO emissions and transport, in *Global Biomass Burning Atmospheric, Climatic, Biospheric Implications*, edited by J. S. Levine, pp. 147–154, MIT Press, Cambridge, Mass., 1991b.

Connors, V. S., M. Flood, T. Jones, B. Gromsen, S. Nolf, and H. G. Reichle Jr., Global distribution of biomass burning and carbon monoxide in the middle troposphere during early April and October 1994, in *Biomass Burning and Global Change, Volume 1: Remote Sensing and Modeling of Biomass Burning, and Biomass Burning in the Boreal Forest*, edited by J. S. Levine, pp. 99–106, MIT Press, Cambridge, Mass., 1996.

Connors, V. S., B. B. Gormsen, S. Nolf, and H. G. Reichle Jr., Spaceborne observations of the global distribution of carbon monoxide in the middle troposphere during April and October 1994, *J. Geophys. Res.*, *104*, 21,455–21,470, 1999.

Conway, T. J., P. P. Trans, L. S. Waterman, K. W. Thoning, D. R. Kitzis, K. A. Masarie, and N. Zhang, Evidence for interannual variability of the carbon cycle from the NOAA/CMDL global air sampling network, *J. Geophys. Res.*, *99*, 22,832–22,855, 1994.

Crutzen, P. J., and M. O. Andreae, Biomass burning in the tropics: Impact on atmospheric chemistry and biogeochemical cycles, *Science*, *250*, 1669–1678, 1990.

Crutzen, P. J., L. E. Heidt, J. P. Krasnec, and W. H. Pollock, Biomass burning as a source of atmospheric gases CO, H$_2$, N$_2$O, NO, CH$_3$Cl and COS, *Nature*, *282*, 253–256, 1979.

DeSouza-Machado, S., L. Strow, and S. Hannon, kCompressed atmospheric radiative transfer algorithm (kCARTA), in *Satellite Remote Sensing of Clouds and the Atmosphere, Proceedings of the European Symposium on Aerospace Remote Sensing 3220, Europto Series*, Inst. of Electr. Eng., London, 1997.

Dickerson, R. R., and A. C. Delany, Modification of a commercial gas filter correlation CO detector for enhanced sensitivity, *J. Atmos. Oceanic Technol.*, *5*, 424–431, 1988.

Doddridge, B. G., P. A. Dirmeyer, J. T. Merrill, S. J. Oltmans, and R. R. Dickerson, Interannual variability over the eastern North Atlantic Ocean: Chemical and meteorological evidence for tropical influence on regional-scale transport in the extratropics, *J. Geophys. Res.*, *99*, 22,923–22,935, 1994.

Doddridge, B. G., R. Morales-Morales, K. P. Rhoads, J. T. Merrill, P. C. Novelli, R. R. Dickerson, V. S. Connors, and H. G. Reichle Jr., Ground-based and airborne observations of carbon monoxide during NASA Measurements of Air Pollution From Satellite (MAPS) missions SRL-1 and SRL-2, *J. Geophys. Res.*, *103*, 19,305–19,316, 1998.

Freiman, M. T., M. R. Jury, and S. Medcalf, The state of the atmosphere over South Africa during the Southern African Regional Science Initiative (SAFARI 2000), *S. Afr. J. Sci.*, *98*, 91–98, 2002.

Goode, J. G., R. J. Yokelson, D. E. Ward, R. A. Susott, R. E. Babbitt, M. A. Davies, and W. M. Hao, Measurement of excess O$_3$, CO$_2$, CO, CH$_4$, C$_2$H$_4$, C$_2$H$_2$, HCN, NO, NH$_3$, HCOOH, CH$_3$COOH, HCHO, and CH$_3$OH in 1997 Alaskan biomass burning plumes by airborne Fourier transform infrared spectroscopy (AFTIR), *J. Geophys. Res.*, *105*, 22,147–22,166, 2000.

Harriss, R. C., et al., Carbon monoxide and methane over Canada, July–August 1990, *J. Geophys. Res.*, *99*, 1659–1669, 1994.

Haywood, J. M., S. R. Osborne, P. N. Francis, A. Keil, P. Formenti, and M. O. Andreae, The mean physical and optical properties of biomass burning aerosol measured by the C-130 aircraft during SAFARI-2000, *J. Geophys. Res.*, *108*, doi:10.1029/2002JD002226, in press, 2003.

Herman, J. R., P. K. Bhartia, O. Torres, C. Hsu, C. Seftor, and E. Celarier, Global distribution of UV-absorbing aerosols from Nimbus 7/TOMS data, *J. Geophys. Res.*, *102*, 16,911–16,922, 1997.

Hobbs, P. V., P. Sinha, R. J. Yokelson, T. J. Christian, D. R. Blake, S. Gao, T. W. Kirchstetter, T. Novakov, and P. Pilewskie, Evolution of gases and particles from a savanna fire in South Africa, *J. Geophys. Res.*, *108*, doi:10.1029/2002JD002352, in press, 2003.

Huang, H. L., and P. Antonelli, Application of principal component analysis to high-resolution infrared measurement compression and retrieval, *J. Appl. Meteorol.*, *40*, 365–388, 2001.

Jonquiéres, I., and A. Marenco, Redistribution by deep convention and long-range transport of CO and CH$_4$ emissions from the Amazon basin, as observed by the airborne campaign TROPOZ II during the wet season, *J. Geophys. Res.*, *103*, 19,075–19,091, 1998.

Kaufman, Y. J., A. Setzer, D. Ward, D. Tanre, B. N. Holben, P. Menzel, M. C. Pereira, and R. Rasmussen, Biomass burning airborne and space-borne experiment in the Amazonas (BASE-A), *J. Geophys. Res.*, *97*, 14,581–14,599, 1992.

Khalil, M. A. K., and R. A. Rasmussen, Carbon monoxide in the Earth's atmosphere: Indications of a global increase, *Nature*, *332*, 242, 1988.

Khalil, M. A. K., and R. A. Rasmussen, The global decrease of carbon monoxide and its causes (abstract), *Eos Trans. AGU*, *75*(14), 87, Spring Meet., 1994.

Kirkman, G. A., S. J. Piketh, M. O. Andreae, G. Helas, and H. J. Annegarn, Distribution of aerosols, ozone, and carbon monoxide over southern Africa, *S. Afr. J. Sci.*, *96*, 423–431, 2000.

Lang, P. M., L. P. Steele, L. S. Waterman, R. C. Martin, K. A. Masarie, and E. J. Dlugokencky, NOAA/CMDL atmospheric methane data for the period 1983–1990 from shipboard flask sampling, *Tech. Rep.*, NOAA, Silver Spring, Md., 1992.

Law, K. S., and J. A. Pyle, Modeling trace gas budgets in the troposphere, 2, CH$_4$ and CO, *J. Geophys. Res.*, *98*, 18,401–18,412, 1993.

Lindesay, J. A., M. O. Andreae, J. G. Goldammer, G. Harris, H. J. Annegarn, M. Garstang, R. J. Scholes, and B. W. van Wilgen, International Geosphere-Biosphere Programme/International Global Atmospheric Chemistry SAFARI-92 field experiment: Background and overview, *J. Geophys. Res.*, *101*, 23,521–23,530, 1996.

Logan, J. A., M. J. Prather, S. C. Wofsy, and M. B. McElroy, Tropospheric chemistry: A global perspective, *J. Geophys. Res.*, *86*, 7210–7254, 1981.

McMillan, W. W., L. L. Strow, W. L. Smith, H. E. Revercomb, and H. L. Huang, The detection of enhanced carbon monoxide abundances in remotely sensed infrared spectra of a forest fire smoke plume, *Geophys. Res. Lett.*, *23*, 3199–3202, 1996.

McMillan, W. W., L. L. Strow, W. L. Smith, H. E. Revercomb, H. L. Huang, A. M. Thompson, D. P. McNamara, and W. F. Ryan, Remote sensing of carbon monoxide over the continental United States on September 12–13, 1993, *J. Geophys. Res.*, *102*, 10,695–10,709, 1997.

Moeller, C. C., H. E. Revercomb, S. A. Ackerman, and W. P. Menzel, Evaluation of MODIS thermal IR band L1B radiances during SAFARI-2000, *J. Geophys. Res.*, *108*, doi:10.1029/2002JD002323, in press, 2003.

Newell, R. E., Y. Zhu, V. S. Connors, H. G. Reichle Jr., H. G. Novelli, and B. B. Gormsen, Atmospheric processes influencing measured carbon monoxide in the NASA measurement of air pollution from satellites (MAPS) experiment, *J. Geophys. Res.*, *104*, 21,487–21,501, 1999.

Novelli, P. C., L. P. Steele, and P. P. Tans, Mixing ratios of carbon monoxide in the troposphere, *J. Geophys. Res.*, *97*, 20,731–20,750, 1992.

Novelli, P. C., K. A. Masarie, P. P. Tans, and P. M. Lang, Recent changes in atmospheric carbon monoxide, *Science*, *263*, 1587–1590, 1994.

Novelli, P. C., K. A. Masarie, and P. M. Lang, Distributions and recent trends of carbon monoxide in the lower troposphere, *J. Geophys. Res.*, *103*, 19,015–19,033, 1998a.

Novelli, P. C., et al., An internally consistent set of globally distributed atmospheric carbon monoxide mixing ratios developed using results from an intercomparison of measurements, *J. Geophys. Res.*, *103*, 1285–1293, 1998b.

Otter, L. B., L. Marufub, and M. C. Scholes, Biogenic biomass biofuel sources of trace gases in southern Africa, *S. Afr. J. Sci.*, *97*, 131–138, 1997.

Otter, L. B., et al., The Southern African Regional Science Initiative (SAFARI 2000): Wet season campaigns, *S. Afr. J. Sci.*, *98*, 131–137, 2002.

Pak, B. C., and M. J. Prather, CO_2 source inversions using satellite observations of the upper troposphere, *J. Geophys. Res.*, *24*, 4571–4574, 2001.

Pickering, K. E., et al., Convective transport of biomass burning emissions over Brazil during TRACE-A, *J. Geophys. Res.*, *101*, 23,993–24,012, 1996.

Piketh, S. J., H. J. Annegarn, and P. D. Tyson, Lower tropospheric aerosol loading over South Africa: The relative contribution of aeolian dust, industrial emissions, and biomass burning, *J. Geophys. Res.*, *104*, 1597–1607, 1999.

Pougatchev, N. S., et al., Ground-based infrared solar spectroscopic measurements of carbon monoxide during 1994 Measurement of Air Pollution from Space flights, *J. Geophys. Res.*, *103*, 19,317–19,325, 1998.

Pougatchev, N. S., et al., Pacific Exploratory Mission-Tropics carbon monoxide measurements in historical context, *J. Geophys. Res.*, *104*, 26,195–26,207, 1999.

Reichle, H. G., Jr., et al., Carbon monoxide measurements in the troposphere, *Science*, *218*, 1024–1026, 1982.

Reichle, H. G., Jr., V. S. Connors, J. A. Holland, W. D. Hypes, H. A. Wallio, J. C. Casas, B. B. Gormsen, M. S. Saylor, and W. D. Hesketh, Middle and upper tropospheric carbon monoxide mixing ratios as measured by a satellite-borne remote sensor during November 1981, *J. Geophys. Res.*, *91*, 10,865–10,887, 1986.

Reichle, H. G., Jr., V. S. Connors, J. A. Holland, R. T. Sherrill, H. A. Wallio, J. C. Casas, E. P. Condon, B. B. Gormsen, and W. Seiler, The distribution of middle tropospheric carbon monoxide during early October 1984, *J. Geophys. Res.*, *95*, 9845–9856, 1990.

Reichle, H. G., Jr., and V. S. Connors, The mass of CO in the atmosphere during October 1984, April 1994, and October 1994, *J. Atmos. Sci.*, *56*, 307–310, 1999.

Reichle, H. G., Jr., et al., Space shuttle based global CO measurements during April and October 1994, MAPS instrument, data reduction, and data validation, *J. Geophys. Res.*, *104*, 21,443–21,454, 1999.

Roths, J., and G. W. Harris, The tropospheric distribution of carbon monoxide as observed during the TROPOZ II experiment, *J. Atmos. Chem.*, *24*, 157–188, 1996.

Scheel, H. E., E. G. Brunke, R. Sladkovic, and W. Seiler, In situ CO concentrations at the sites Zugspitze (47°N, 11°E) and Cape Point (34°S, 18°E) in April and October 1994, *J. Geophys. Res.*, *103*, 19,295–19,304, 1998.

Scholes, R. J., D. E. Ward, and C. O. Justice, Emissions of trace gases and aerosol particles due to vegetation burning in Southern Hemisphere Africa, *J. Geophys. Res.*, *101*, 23,677–23,682, 1996.

Sherwood, S., A microphysical connection among biomass burning, cumulus clouds, and stratospheric moisture, *Science*, *295*, 1272–1275, 2002.

Sinha, P., P. V. Hobbs, R. J. Yokelson, I. T. Bertschi, D. R. Blake, I. J. Simpson, S. Gao, T. W. Kirchstetter, and T. Novakov, Emissions of trace gases and particles from savanna fires in southern Africa, *J. Geophys. Res.*, *108*, doi:10.1029/2002JD002325, in press, 2003.

Stearns, J. R., M. S. Zahniser, C. E. Kolb, and B. P. Sandford, Airborne infrared observations and analyses of a large forest fire, *Appl. Opt.*, *25*, 2554–2562, 1986.

Strow, L., H. Motteler, R. Benson, S. Hannon, and S. De Souza-Machado, Fast computation of monochromatic infrared atmospheric transmittances using compressed look-up tables, *J. Quant. Spectrosc. Radiat. Transfer*, *59*, 481–493, 1998.

Strow, L. L., D. Tobin, and S. Hannon, Line mixing in the Π-Δ CO_2 Q-branch at 740 cm^{-1}, in *Atmospheric Spectroscopy Applications*, Reims, France, 1993.

Swap, R. J., H. J. Annegarn, and L. Otter, Southern African Regional Science Initiative: SAFARI 2000: Condensed science plan, *S. Afr. J. Sci.*, *98*, 131–137, 2002a.

Swap, R. J., et al., The Southern African Regional Science Initiative (SAFARI 2000): Dry-season field campaign: An overview, *S. Afr. J. Sci.*, *98*, 125–130, 2002b.

Sze, N. D., Anthropogenic CO emissions: Implications for atmospheric CO-OH-CH_4 cycle, *Science*, *195*, 673–675, 1977.

Thompson, A., B. G. Doddridge, J. C. Witte, R. D. Hudson, W. T. Luke, J. E. Johnson, B. J. Johnson, S. J. Oltmans, and R. Weller, A tropical Atlantic paradox: Shipboard and satellite views of a tropospheric ozone maximum and wave-one in January–February 1999, *Geophys. Res. Lett.*, *27*, 3317–3320, 2000.

Thompson, A., J. C. Witte, R. D. Hudson, H. Guo, J. R. Herman, and M. Fujiwara, Tropical tropospheric ozone and biomass burning, *Science*, *291*, 2128–2132, 2001.

Thompson, A. M., K. E. Pickering, D. P. McNamara, M. R. Schoeberl, R. D. Hudson, J. H. Kim, E. V. Browell, V. W. J. H. Kirchhoff, and D. Nganga, Where did tropospheric ozone over southern Africa and the tropical Atlantic come from in October 1992? Insights from TOMS, GTE TRACE A, and SAFARI 1992, *J. Geophys. Res.*, *101*, 24,251–24,278, 1996.

Thompson, O., Regularizing the satellite temperature-retrieval problem through singular-value decomposition of the radiative transfer physics, *Mon. Weather Rev.*, *120*, 2314–2328, 1992.

Torres, O., P. Bhartia, J. R. Herman, Z. Ahmad, and J. Gleason, Derivation of aerosol properties from satellite measurements of backscattered ultraviolet radiation: Theoretical basis, *J. Geophys. Res.*, *103*, 17,099–17,110, 1998.

Wang, J. C., J. Gille, H. E. Revercomb, and V. P. Walden, Validation study of the MOPITT retrieval algorithm: Carbon monoxide retrieval from IMG observations during WINCE, *J. Atmos. Oceanic Technol.*, *17*, 1285–1296, 2000.

Wilson, S. H. S., N. C. Atkinson, and J. A. Smith, The development of an airborne infrared interferometer for meteorological sounding studies, *J. Atmos. Oceanic Technol.*, *16*, 1912–1927, 1999.

Worden, H., R. Beer, and C. P. Rinsland, Airborne infrared spectroscopy of 1994 western wildfires, *J. Geophys. Res.*, *102*, 1287–1299, 1997.

Yokelson, R. J., J. G. Goode, D. E. Ward, R. A. Susott, R. E. Babbitt, D. D. Wade, L. Bertschi, D. W. T. Griffith, and W. M. Hao, Emissions of formaldehyde, acetic acid, methanol, and other trace gases from biomass fires in North Carolina measured by airborne Fourier transform infrared spectroscopy, *J. Geophys. Res.*, *104*, 30,109–30,125, 1999.

Yokelson, R. J., I. T. Bertschi, T. J. Christian, P. V. Hobbs, D. E. Ward, and W. M. Hao, An overview of trace gas measurements in nascent, aged, and cloud-processed smoke from African savanna fires by Airborne Fourier Transform Spectroscopy (AFTIR), *J. Geophys. Res.*, *108*, doi:10.1029/2002JD002322, in press, 2003.

Yurganov, L. N., E. I. Grechko, and A. V. Dzhola, Variations of carbon monoxide density in the total atmospheric column over Russia between 1970 and 1995: Upward trend and disturbances attributed to the influence of volcanic aerosols and forest fires, *Geophys. Res. Lett.*, *24*, 1231–1234, 1997.

————————

T. J. Christian and R. J. Yokelson, Department of Chemistry, University of Montana, Missoula, MT 59812, USA. (byok@selway.umt.edu)

B. G. Doddridge, Department of Meteorology, University of Maryland, College Park, MD 20742, USA. (bruce@atmos.umd.edu)

P. V. Hobbs, Cloud and Aerosol Research Group, Department of Atmospheric Sciences, University of Washington, Box 351640, Seattle, WA 98195, USA. (phobbs@atmos.washington.edu)

R. O. Knuteson and H. E. Revercomb, Cooperative Institute for Meteorological Satellite Studies, University of Wisconsin, 1225 West Dayton Street, Madison, WI 53706, USA. (HankR@ssec.wisc.edu; robert.knuteson@ssec.wisc.edu)

J. V. Lukovich, 685 Fisher Street, Winnipeg, Manitoba, R3L 2K9, Canada,

M. L. McCourt, W. W. McMillan, and L. Sparling, Physics Department, University of Maryland Baltimore County, 1000 Hilltop Circle, Baltimore, MD 21250, USA. (mcmillan@umbc.edu; mmccou1@umbc.edu; sparling@dynatron.umbc.edu)

P. C. Novelli, Climate Monitoring and Diagnostics Laboratory, National Oceanic and Atmospheric Administration (NOAA), DSRC, 325 Broadway, Boulder, CO 80305, USA. (P.C.Novelli@noaa.gov)

S. J. Piketh, Climatology Research Group, University of Witswatersrand, Johannesburg, Private Bag 3x, WITS, 2050, South Africa. (stuart@crg.bpb.wits.ac.za)

D. Stein and R. J. Swap, Department of Environmental Sciences, University of Virginia, P.O. Box 400123, Clark Hall, Charlottesville, VA 22904, USA. (sandals_snow@yahoo.com; rjs8g@maddux.evsc.virginia.edu)